

Advanced laboratory course — University of Siegen

Determination of crystal orientation using x-ray diffraction: The Laue method

Author:

Marcel Roth

`marcel.roth@uni-siegen.de`

Version:

26th April 2007

Contents

1	X-ray radiation	4
1.1	Discovery	4
1.2	Erzeugung	5
1.3	Characterisitics	8
1.4	Detection	8
1.5	Radiation protection	9
2	Beschreibung von Kristallen	10
2.1	Coordinate systems and lattice planes	10
2.2	Reciprocal lattice and Miller's indexes	10
2.2.1	Angle between two lattice planes	12
2.2.2	Interplanar distances	12
2.3	Symmetrie Operations, Bravais lattices and point groups	14
2.4	Stereographic projection	15
2.4.1	Wulff net	16
2.5	Crystal structures and used crystals.	19
2.5.1	Quartz	19
2.5.2	Zinc blend structure	19
3	X-ray diffraction at crystals	21
3.1	Simple diffraction theory	21
3.2	The Laue equations	22
3.3	Ewald construction and the reciprocal space	22
3.4	Bragg's interpretation of the diffraction condition	23
3.5	Atomic form factor, structure factor and extinction rules	24
4	Versuchsbeschreibung	26
4.1	Experimental tasks	26
4.2	Elements of the experiment	28
4.2.1	Safety warnings and instruction rules	28
4.2.2	Laue-camera	29
4.2.3	Laserjustierung	29
4.2.4	Projektionen der Reflexe	30
4.2.5	Filmentwicklung und Imageplate-system	33
4.2.6	Literature of comparable experiments (german)	33
5	References	34

Hint for the linked files:

The PDF files, that are linked inside the manual are contained in the zip-file `addon.zip`. It is downloadable from www.fkp-siegen.de. The contained files have to be stored in the same directory like the manual itself.

1 X-ray radiation

1.1 Discovery

In 1895 Wilhelm Conrad Röntgen investigated the characteristics of gaseous discharge tubes. He noticed that with every gaseous discharge there were fluorescence appearances on a fluorescent screen outside the tube. Röntgen realized that the reason for this had to be a new kind of radiation whose existence had been undiscovered till then. He dated the day of this discovery to 08.11.1895. In the English-speaking literature the term "X-rays", which had been suggested by the discoverer himself, is generally accepted. In the German-speaking region the radiation is named after its discoverer: "Röntgenstrahlung". Röntgen himself carried out the first investigations to determine the characteristics of the new radiation and realized that it was able to pass through optically opaque materials. The proof of the electromagnetic wave-character of the radiation, however, was

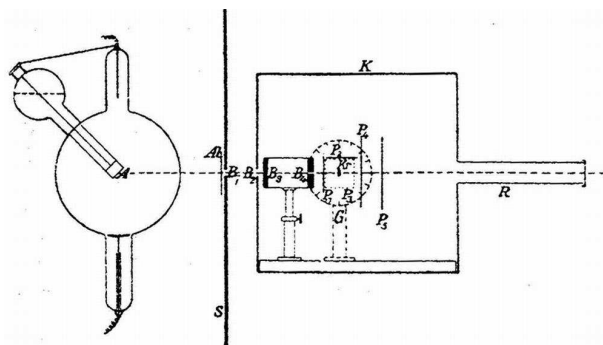


FIG. 1.1: Experimental setup according to Friedrich, Kipping und v. Laue - Quelle: [Lau13]

furnished by Laue, Friedrich and Knipping only in 1912 by diffraction experiments on crystals. FIG. 1.1 shows the historical experimental setup used by Kipping and Friedrich.

As it is described below the x-ray tube created polychromatic x-ray radiation. The outgoing radiation was collimated by holes in two lead plates onto the crystal under investigation. The crystal itself was mounted on a goniometer with some degrees of freedom. The photo plate was used for detection. Two of the published photographs are shown in FIG. 1.2.

The publication of this work took place 1913 in the "Annalen der Physik" and already in 1914 Max von Laue received the Nobel price as initiator of these investigations.

The Laue method is still used with the help of conventional x-ray tubes for determination of the crystal orientation (i.e. the determination of the orientation of the crystallographic base vectors with respect to the outer coordinate system). The availability of synchrotrons as sources of x-ray radiation (extreme high intensity, broad spectrum of frequencies, small divergence) enlarged the perspectives of the Laue-Method towards a time-resolved determination of the crystal structure. The basic knowledge, that is also necessary in this experiment, is also for these applications inevitable.

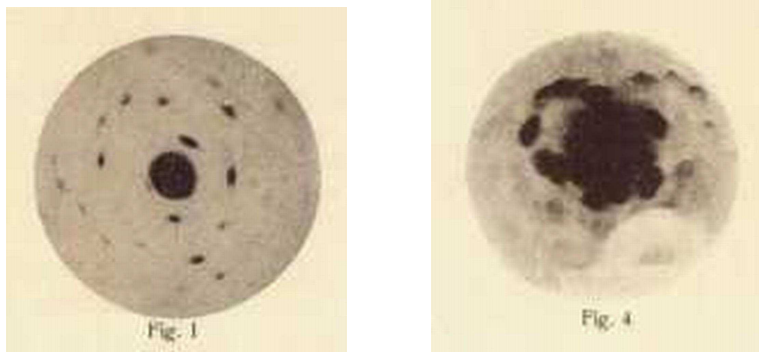


FIG. 1.2: Historische Laue-Aufnahmen eines Kupfervitrolkristalls

1.2 Erzeugung

X-rays are quanta of electromagnetic fields in the high energy range; they have a wavelength between 1 pm and 1 nm. This corresponds to an energy value between 1 MeV up to 1 keV.

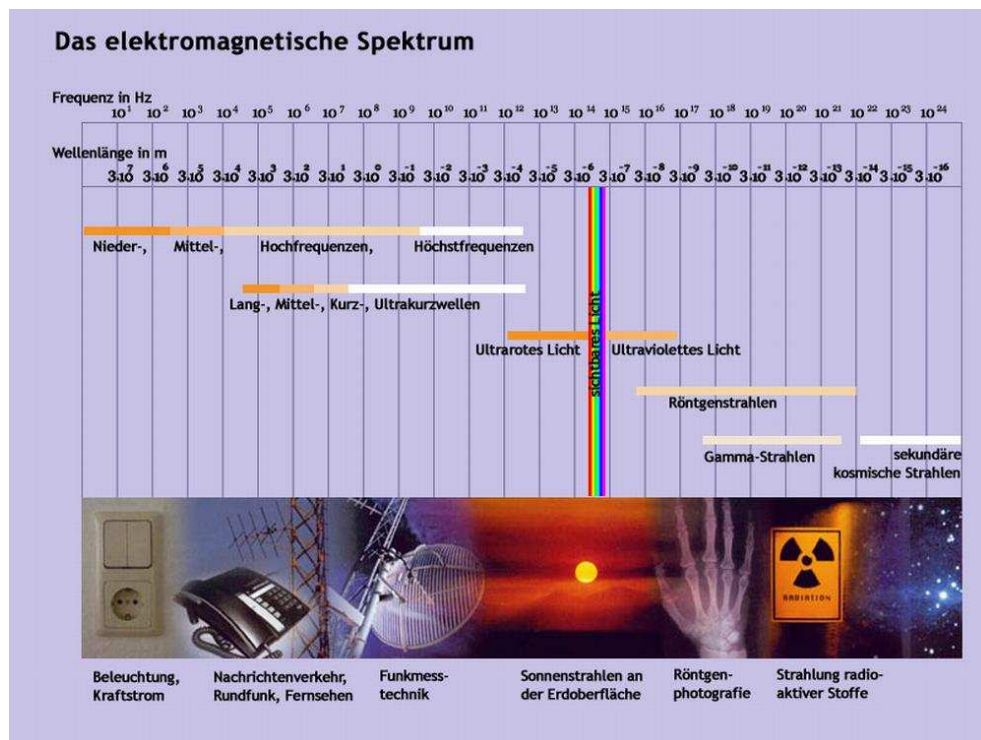


ABB. 1.3: Elektromagnetisches Spektrum; Quelle: "Gebändigtes Licht", Themenheft der DPG und des BMBF, 06/2000

In the electromagnetic spectrum (1.3) the lower energies beyond this are so-called hard ultraviolet rays; the energies above 100 keV are called gamma rays, if the radiation is generated through nuclear transitions.

X-rays have a relatively high energy compared to visible light and that is why they can easily penetrate material. Furthermore, X-rays can induce materials to fluorescence and they can blacken photographic plates. Because of these characteristics the X-ray methods found wide application in medicine and technology.

Electromagnetic radiation is created, if charged particles are accelerated. This happens for example in a synchrotron by deflection of the electrons in magnetic fields or by a simple deceleration of electrons in a solid material as it is the case for the x-ray tube. FIG. 1.4 shows such an x-ray

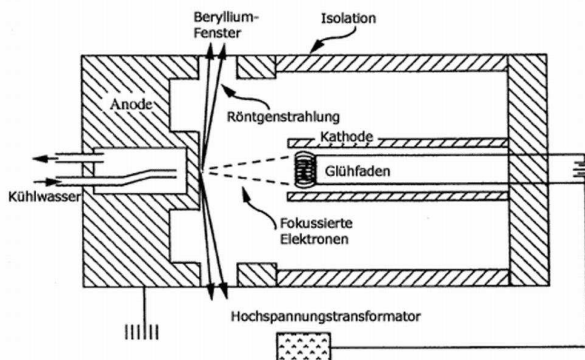


FIG. 1.4: Principal setup of a x-ray tube

tube. Free electrons are liberated at the cathode by means of glow emission and then accelerated in a high voltage field (10 kV-300 kV). When these electrons hit the anode, they will be decelerated in one or several hits with bound and free atomic electrons. The fast electrons transfer a certain amount of momentum and kinetic energy to the atomic electrons:

$$E_{\text{kin}} = \frac{1}{2} m_e \cdot v^2 = e \cdot U \quad (1.1)$$

A certain part of this energy will be emitted as x-ray radiation. However, the biggest part of the energy causes a heating of the anode material. Anode material as its melting temperature is higher than 3000° C. In order to increase the radiation intensity or just to prevent a melting of the anode material, the anode has to be water cooled. Copper, molybden, silver or chromium are common anode materials. Because of absorption in air yield of the x-ray Bremsstrahlung intensity is maximal for copper radiation.

A theoretical description of this “Bremsstrahlung” is done with the help of the so called Lienard-Wiechert potential:

$$\varphi(\mathbf{x}, t) = \int_V \int \frac{\rho(\mathbf{x}', t')}{|\mathbf{x} - \mathbf{x}'|} \cdot \delta(t' - t - \frac{|\mathbf{x} - \mathbf{x}'|}{c}) d\mathbf{x}' dt \quad (1.2)$$

For a single electric charge this potential can be calculated analytically and one gets the following

radiation fields:

$$\mathbf{E}(\mathbf{x}, t) = \frac{e}{c^2} \left[\frac{1 - \beta}{R - \vec{\beta} \cdot \mathbf{R}} (\mathbf{R} - \vec{\beta} \cdot R) + \frac{\mathbf{R} \times (\mathbf{R} \times (\vec{\beta} \cdot R) \times \dot{\mathbf{v}})}{R - \vec{\beta} \cdot \mathbf{R}} \right] \quad (1.3)$$

$$\mathbf{B}(\mathbf{x}, t) = \frac{\mathbf{R}}{R} \times \mathbf{E}(\mathbf{x}, t) \quad (1.4)$$

with $\mathbf{R} = \mathbf{x} - \mathbf{x}' = \mathbf{x} - \mathbf{r}(t')$ and $\beta = v/c$ as the velocity of the electrons normalised to the speed of light. In the case of Bremsstrahlung radiation the contribution $\vec{\beta} \times \dot{\mathbf{v}}$ vanishes and the absolute value of the corresponding Poynting-Vektor is given by:

$$|\mathbf{S}| = S = \frac{c}{4\pi} \frac{e^2}{c^4} \frac{\dot{v}^2}{R^2} \cdot \frac{\sin^2(\vartheta)}{(1 - \beta \cdot \cos(\vartheta))^6} \quad (1.5)$$

Here ϑ is the angle to the propagation direction of the electrons in the x-ray tube. The function

$$\begin{matrix} \beta_1 < \beta_2 < \beta_3 \\ U_3 < U_2 < U_1 \end{matrix}$$

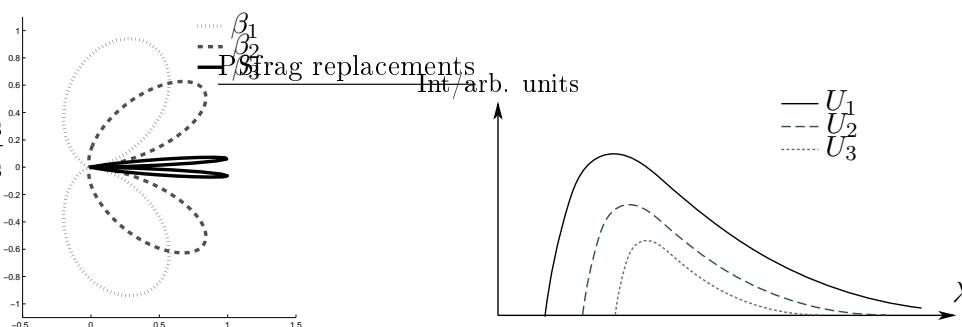


FIG. 1.5: Characteristics of Bremsstrahlung radiation

(1.5) is depicted in FIG. 1.5 for three different values of β . Furthermore a schematic drawing of the emitted spectrum is shown. From (1.1) one can see, that there is a cutoff wavelength λ_{\min} in the left part of the spectrum, that is related to maximum kinetic energy of the Elektronen, that are decelerated in the anode. Photons with this wavelength are created, if the total kinetic energy of the electrons (1.1) is used for the production of the photon. One gets:

$$\begin{aligned} \lambda_{\min} &= \frac{2\pi \cdot \hbar c}{\hbar \omega} \\ &= \frac{2\pi \cdot \hbar c}{E_{\text{kin}}} \\ \lambda_{\min} &= \frac{2\pi \cdot \hbar c}{eU} \end{aligned} \quad (1.6)$$

$$\Rightarrow \lambda_{\min}[\text{\AA}] \approx \frac{12,4}{U[\text{keV}]} \quad (1.7)$$

The spectrum of the Bremsstrahlung is covered with the so called characteristic spectrum. It originated from accelerated electrons, that liberate atomic electrons in the anode material. What

remains is an excited atom, which returns to its ground state by catching an free electron and emitting an photon. This anode material specific radiation has a limited spektral bandwidth and so it is very bright. This part of the total radiation power is of lower interest in this experiment. However, it might explain, why certain diffraction spots have a very high intensity.

1.3 Characterisitics

As already mentioned, Röntgen discovered that X-rays penetrates deeper into matter than light because of its high energy. To describe the interaction between X radiation and matter adequately, the following effects have to be examined: absorption, scattering, generation of secondary radiation, pair production, ionization, luminescence as well as diffraction and refraction. Here only the last two effects will be looked at more closely because they are essential for the understanding of the Laue method. For questions concerning the other effects we refer to the teaching module "X-ray optics" and to the relevant literature. [Gru94].

To observe diffraction effects, the wavelength of the radiation and the measurements of the object on which the radiation is to be diffracted have to be of the same order of magnitude. In the range of "visible light" we deal with wavelengths between 400 and 700nm. The typical measurements of a diffraction lattice have to be of the same scale and thus ruled gratings typically have some 1000 lines/nm. The intervals between the lines of a diffraction lattice for the X-ray range then would be of the same magnitude as the distance between the atoms because the wavelength is typically 1000 times smaller than in the visible optical range. A lattice of this kind cannot be artificially produced but the atoms of a crystal form the lattice themselves. Max von Laue, W. Friedrich and P. Knipping recognized this connection already in 1912 [2a]. In their historical experiment they recorded the first diffraction images of crystals in the X-ray range. If a crystal (which functions as a three-dimensional lattice here) is radiated with polychromatic radiation, this radiation will be refracted under different angles depending on the wavelength. (This process is analogous to the process on an optical lattice.) This can be illustrated by the help of the following model: The X-ray field induces each electron within the crystal to oscillate. In this way every electron itself becomes the starting point of X radiation. The electrons, however, do not oscillate automatically in-phase. Because of their different position within the crystal they are hit by the primary radiation at different points of time. There have to be special conditions for the wave trains of the secondary radiation to superpose in constructive ways. That is why the interference conditions are similar to the ones in the optical range. In our case, however, the interference conditions are more complicated because of the three-dimensional lattice structure. The formation of the atoms within the crystal and the positioning of the crystal lattice towards the primary rays are of special importance. The Laue method makes use of this fact to determine the symmetry characteristics of the crystals. We will have a closer look at the particular connections and the formation of diffraction images later.

1.4 Detection

X radiation can be proved by every measurable interaction between X-rays and matter. For example, X radiation ionizes the molecules of the air and in this way indirectly causes the reduction of an electric field between two plates of a capacitor by penetrating the air between those plates. This principle is also used for the Geiger counter after Geiger and Mueller. Here, however, we have an axially symmetric positioning of the capacitor in an inhomogeneous electric field (tube

filled with inert gas under low pressure). The high voltage of the capacitor accelerates every ion which is produced through X radiation. These ions in turn produce free charge carriers through collision ionization and in this way reduce the detection limit for the dose of radiation. By means of such a measurement only the intensity of the X radiation can be examined, a spectral or local resolution is not automatically possible.

The scintillation counter is based on another principle. Here the X-rays induce processes of luminescence within a crystal (usually sodiumiodide doped with thallium). The optical photons generated in this way hit a photocathode and release electrons in this cathode. These electrons are strengthened through a voltage cascade (photomultiplier). Because the strength of the voltage impulse depends on the energy of the X-rays, not only the radiation intensity but also the spectral distribution can be detected, if the decay time of the crystal is short enough. In the Laue method position sensitive area detectors like the following are necessary to detect the diffracted radiation:

- A luminescent screen is exposed to the radiation. The screen transfers the radiation into the optical frequency range, so it can be photographed. However, this method became obsolete and is not used nowadays.
- A photoemulsion is exposed to the radiation. Depending of the structure of the film the processes that leads to a blackening of the film by x-rays are similar to these in the optical range. However, the blackening curve i.e. the connection between lightening time and the degree of blackening is different for x-rays.
- The Laue picture is enhanced by a image signal enhancer and picked up by a CCD- Kamera. So the Laue record is immediately given as an electronic medium.
- The "Imageplate system" is comparable to the detection method by a photo emulsion. The image plate consists of a polymer, in which x-rays can create defects. These defects are stable under normal conditions, but show fluorescence for a characteristic wavelength. With the help of a special scanner the diffraction pattern can be digitalised.

1.5 Radiation protection

Dealing with X-rays is very dangerous. There can be both physical and genetic (hereditary) damages and injuries. Only severe radiation injuries can be perceived immediately by the person affected. That is why special precautionary measures are necessary which are legally regulated in the "Regulation about the Protection against Damages and Injuries caused by X-rays" of January 8th 1987, latest update on July 18th 2002. Because of this regulation there are special guidelines for dealing with X-rays in working environments and supervision. The following measurements and limits guarantee the observance of these legal regulations in our experiment: The maximal local dosage in this experiment was $30 \mu\text{Sv/h}$. The hands will be exposed to radiation about three to five hours if the experiment is well prepared. The limit of radiation for the hands of people dealing with radiation because of their work is 150 mSv/year . So in our Laue experiment the radiation is far beneath the legal limits. The other parts of the body are protected by lead so there is no measurable radiation.

Further information is given in the standard literature.

2 Beschreibung von Kristallen

As indicated in the subsection 1.3, regular submicroscopic structures are necessary for the creation of diffraction pattern with X-ray radiation. Such a regularity has to cover a wide volume area compared to the atomic distances in order to develop strong interference phenomena. Amorphous solid structures do not show regularity and therefore reveal if any only weak interference patterns. On the other hand crystals exhibit even in makroscopic samples very regular structures and can be analysed with X-ray diffraction very efficiently. The description of the different crystal systems and the contained symmetry characteristics is the topic of this section.

2.1 Coordinate systems and lattice planes

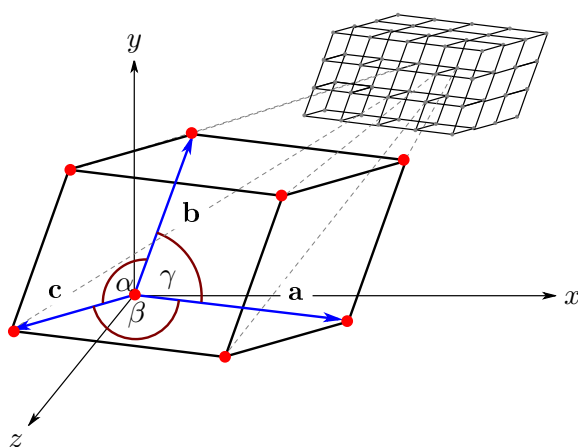


FIG. 2.1: Crystallographic unit cell of a crystal: The basis vectors entitles with \mathbf{a} , \mathbf{b} , \mathbf{c} or $[\mathbf{a}_1, \mathbf{a}_2, \mathbf{a}_3]$. \mathbf{a} and \mathbf{b} enclose the angle γ , \mathbf{b} and \mathbf{c} the angle α and \mathbf{c} and \mathbf{a} the angle β . The lengths of the basis vectors are also called lattice parameters.

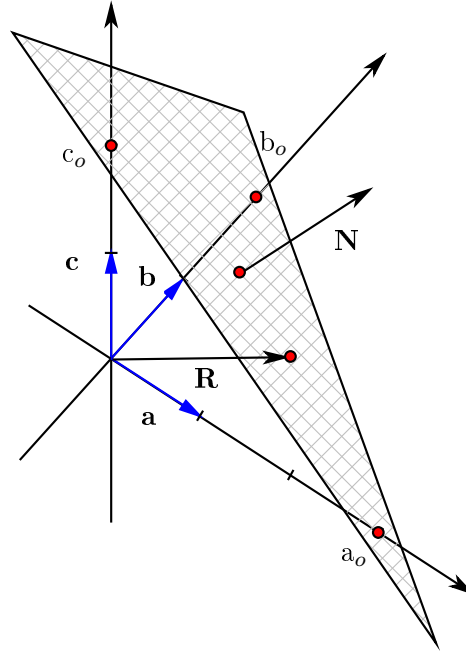
Regularity of a crystal means, that a certain configuration of atoms (a lattice point) in a crystal is repeated over and over again in each of the directions in space to build up the crystal lattice. The smallest configuration of lattice points to build up the whole crystal is called a *crystallographic unit cell* (see FIG. 2.1). Within this unit cell the edges define the by the so called *basis vectors* of the crystal. Now, the periodicity of the crystal demands for a reconstruction of the total crystal by means of successive *translation* in the directions of the three basis vectors.

Neither in nature nor in the laboratory the shape of a macroscopic crystal will exhibit the shape of the unit cell. The outer surfaces of crystals can be classified by certain *lattice planes* instead. These cuts through the crystal, for which the condition of periodicity is given, will cross the axis which are defined by the directions of the basis vectors in the points a_o , b_o und c_o (see FIG. 2.2). It should be mentioned here that a_o , b_o und c_o need not be integer numbers. However, these three numbers are mostly given by interger numbers.

2.2 Reciprocal lattice and Miller's indexes

The reciprocal lattice is a mathematical construction, which is useful for indexing of lattice planes and for further insight to the X-ray diffraction of crystals.

FIG. 2.2: Lattice plane of a crystal: The lattice plane shown in the sketch crosses the extensions of the basis vectors in the points a_o , b_o and c_o (in units of the basis vectors). Equally oriented lattice planes show a constant ratio $a_o:b_o:c_o$. \mathbf{R} is arbitrary vector guiding from the origin to the lattice plane and \mathbf{N} is the normalised vector on the lattice plane.



Die basis vectors of reciprocal lattice are defined by the following equations:

$$\begin{aligned}
 \mathbf{a} \cdot \mathbf{a}^* &= 2\pi & \mathbf{b} \cdot \mathbf{b}^* &= 2\pi & \mathbf{c} \cdot \mathbf{c}^* &= 2\pi \\
 \mathbf{b} \cdot \mathbf{a}^* &= 0 & \mathbf{c} \cdot \mathbf{b}^* &= 0 & \mathbf{a} \cdot \mathbf{c}^* &= 0 \\
 \mathbf{c} \cdot \mathbf{a}^* &= 0 & \mathbf{a} \cdot \mathbf{b}^* &= 0 & \mathbf{b} \cdot \mathbf{c}^* &= 0
 \end{aligned} \tag{2.1}$$

A solution to this linear equation system is given by the definition equations:

$$\begin{aligned}
 \mathbf{a}^* &= \frac{2\pi}{V_{EZ}} \cdot \mathbf{b} \times \mathbf{c} \\
 \mathbf{b}^* &= \frac{2\pi}{V_{EZ}} \cdot \mathbf{c} \times \mathbf{a} \\
 \mathbf{c}^* &= \frac{2\pi}{V_{EZ}} \cdot \mathbf{a} \times \mathbf{b}
 \end{aligned} \quad \text{mit } V_{EZ} = \mathbf{a} \cdot (\mathbf{b} \times \mathbf{c}) \tag{2.2}$$

$$\tag{2.3}$$

Since the basis vectors of the real lattice are linear independent the basis vectors of the reciprocal lattice have the same characteristic and one can develop any vector in terms of these two sets of basis vectors. So one can write $\mathbf{R} = u \cdot \mathbf{a} + v \cdot \mathbf{b} + w \cdot \mathbf{c}$ with suitable values for u , v and w . This arbitrary vector connects the origin with the lattice plane in FIG. 2.2. $\mathbf{N} = \frac{1}{2\pi} \cdot (n_1 \cdot \mathbf{a}^* + n_2 \cdot \mathbf{b}^* + n_3 \cdot \mathbf{c}^*)$ is the normalised vector on the plane.

The perpendicular distance D of the lattice plane to the origin is given by:

$$D = \mathbf{R} \cdot \mathbf{N} = n_1 \cdot u + n_2 \cdot v + n_3 \cdot w \tag{2.4}$$

This equation is valid for all vectors \mathbf{B} leading from the origin to the lattice plain and therefore one can modify (2.4) with respect to the three crossings with the coordinate system axes:

$$D = n_3 \cdot \mathbf{a}_o = n_2 \cdot \mathbf{b}_o = n_1 \cdot \mathbf{c}_o \tag{2.5}$$

The four equations (2.4) and (2.5) together build up the lattice plain equation:

$$h u + k v + l w = m \tag{2.6}$$

Here h, k and l are integer numbers. They are given by $\frac{m}{a_0}, \frac{m}{b_0}$ and $\frac{m}{c_0}$ respectively with a suitable value of m which is also integer. One can show, that (2.6) is the mathematical description of the m th lattice plane, counting from the lattice plane, that includes the origin. The vector

$$\mathbf{G} = h \cdot \mathbf{a}^* + k \cdot \mathbf{b}^* + l \cdot \mathbf{c}^* \tag{2.7}$$

is a arbitrary *reciprocal lattice vector* and is perpendicular on the lattice plane under consideration. It characterises the lattice plane completely using equation (2.6). The triple $(h k l)$ is called as a *Miller's index*. FIG. 2.3 shows three examples for lattice planes together with their Miller's indexes.

2.2.1 Angle between two lattice planes

The angle between two lattice planes is equal to the angle between the corresponding normals on the planes. Therefore equation

$$\cos(\psi) = \frac{\mathbf{G}_1 \cdot \mathbf{G}_2}{G_1 G_2} \tag{2.8}$$

is valid.

2.2.2 Interplanar distances

Moreover the interpretation of the integer number m makes it possible to calculate the *interplanetary distance* between two lattice planes with the same orientation. In a quadratic form one gets:

$$d_{hkl}^2 = \frac{1}{G_{hkl}^2} = \frac{1}{(h \cdot \mathbf{a}^* + k \cdot \mathbf{b}^* + l \cdot \mathbf{c}^*)^2} \tag{2.9}$$

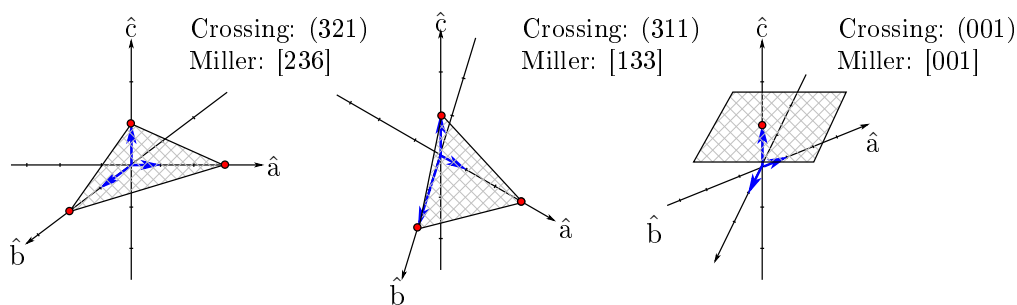
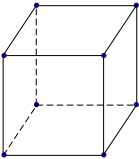
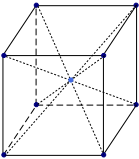
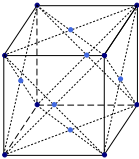
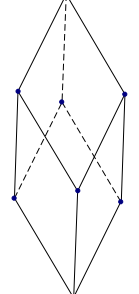
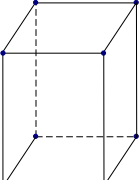
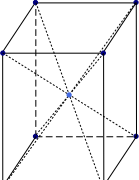
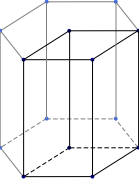
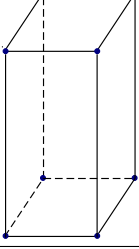
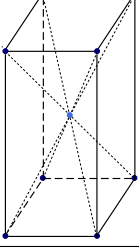
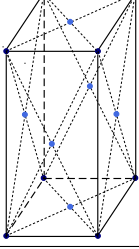
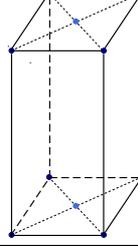
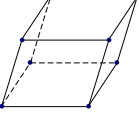
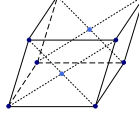
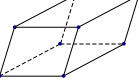


ABB. 2.3: Example of three lattice planes with the corresponding Miller'S indexes. The basis vectors are different for the three cases, so the comparison of the indexes is not sufficient for the comparison of the lattice planes.

Coordinate system attributes	simple	body centered	face face centered	base
cubic $a = b = c$ $\alpha = \beta = \gamma = 90^\circ$				
trigonal $a = b = c$ $\alpha = \beta = \gamma$			For $\alpha = \beta = \gamma = 60^\circ$ the trigonal lattice is equal to the face centered cubic cell	
tetragonal $a = b \neq c$ $\alpha = \beta = \gamma = 90^\circ$				
hexagonal $a = b \neq c$ $\alpha = \beta = 90^\circ$ $\gamma \neq 90^\circ$				
orthorhombic $a \neq b \neq c$ $\alpha = \beta = \gamma = 90^\circ$				
monoclinic $a \neq b \neq c$ $\alpha = \gamma = 90^\circ \neq \beta$				
triclinic $a \neq b \neq c$ $\alpha \neq \beta \neq \gamma$				

TAB. 2.1: The 14 Bravais lattices: For identification of the lattice constants and angles see also FIG. 2.1

2.3 Symmetrie Operations, Bravais lattices and point groups

Symmetry operations are transformations of a system, that remain the system unchanged. The symmetry operation *translation* is the basic transformation, that is valid for every crystal. Beside this there are the following *symmetry operations*:

- Mirror planes (\bar{m}): The system has a mirror plane with a certain orientation.
- Rotation (2, 3, 4, 6): There are 2,3, 4 and 6 fold rotation axes, i.e. the system turns to itself by rotation of $360^\circ/x$.
- Inversion ($\bar{1}$): The inversion inverts all spacial coordinates.

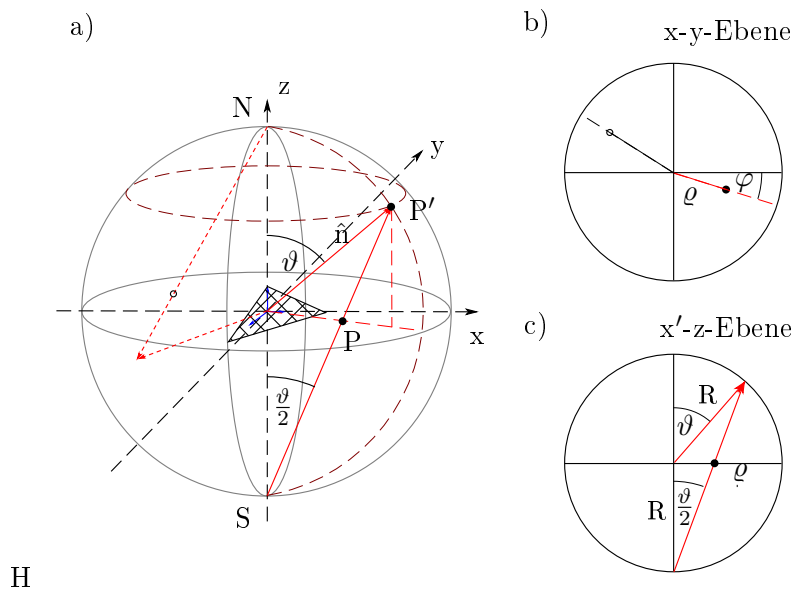
These symbols appear in groups of 1, 2 or 3 characters. The interpretation of a single character is easy. For instance $\bar{6}$ means, that there is a 6-fold axis with a inversion $\bar{1}$, that has to used after each rotation step by 60° . For symbols with 2 characters there are two types. The first type says, that for 43 one has to apply a 3-fold symmetry axis, that is perpendicular to a 4-fold axis. The meaning is different for $4/m$. Now there is a 4-fold axis, that is perpendicular to a mirror plane m . Symbols with 3 characters are understood in the same way as Symbols with 2 characters. However, here one has to use all three directions of space. As seen in the subsections 2.1 and 2.2 it is possible to describe a crystal not only by a single unit cell and single set of basis vectors respectively. There are uncountably many lattice planes, which fulfil the condition of peridicity and therefore can build up the “walls” of other unit cells. However, there are more useful definitions of unit cells and less useful ones. In the end all these unit cells can be reduced to a basic shape of the crystal lattice because of its intrinsic symmetry.

In general one distinguishes between 7 different groups of symmetry operations each of which contains a certain amount of symmetry operations. These groups are $\{\bar{1}, 2/m, mmm, 4/mmm, \bar{3}m, 6/mmm$ und $m\bar{3}m\}$ and represent the 7 coordinate systems, that are shown in TAB. 2.1.

Although the infinite crystal will always show the specific symmetry elements, the symmetry of the unit cell can be reduced by certain configuration of the atoms. Nevertheless one sticks up to the classification into the 7 coordinate systems. The reduced set of symmetry groups are the 32 *point groups* that are listed in TAB. 2.2 with their corresponding coordinate system.

Triklin	Monoklin	Rhombisch	Tetragonal	Trigonal	Hexagonal	Kubisch
$\bar{1}$	$2/m$	mmm	$4/mmm$	$\bar{3}m$	$6/mmm$	$m\bar{3}m$
—	—	$mm2$	$4mm$	$3m$	$6mm$	—
—	—	—	$4/m$	$\bar{3}$	$6/m$	$m\bar{3}$
1	2	222	422	32	622	432
—	m	—	$\bar{4}2m$	—	$\bar{6}m2$	$\bar{4}3m$
—	—	—	4	3	6	23
—	—	—	$\bar{4}$	—	$\bar{6}$	—

TABLE 2.2: 32 kristallographische Punktgruppen unterteilt in die 7 Grundgittertypen



H

FIGURE 2.4: Stereographic projection: a) Shown is a lattice plane or a part of the surface of a crystal. The corresponding pole is P' , P is the point in the projection with the coordinates (φ, ϑ) and (φ, ϱ) respectively. b) Equatorial plane (plane of the stereographic projection) with the definition of the length ϱ . c) The x' - z -projection is the layer, in which the connection line and the pole lie.

2.4 Illustration of point groups und containing symmetries: Stereographic projection

The stereographic projection is used to display the relation between the macroscopic crystal planes and arbitrary lattice planes respectively in a 2dimensional way. Thus, it is necessary to project the points of a sphere into a plane. (for labels and names see FIG. 2.4):

- The crystal is placed in a sphere with a radius of 1 in such a way, that the *equator plane* of the sphere is the plane of the stereographic projection.
- Starting from the centre **Lote** \hat{n} on the crystal planes are drawn up to the surface of the spheres.
- The crossing points of these **Lote** with the surface of the sphere are called surface poles or just poles P' . The poles of the northern hemisphere are connected with the south pole S of the sphere, those of the southern hemissphere with the north pole N . The crossings P with the equatorial plane are directly the points in the stereographic projection with the coordinates (ϑ, φ) or (ϱ, φ) .
- A pole on the northern hemisphere is drawn as a filled circle, pole in the southern hemisphere is drawn as a ring.

2.4.1 Lattice planes and zones in the stereographic projection: The Wulff net

In generell there are two basic methods to display a arbitrary lattice plane in the stereographic projection.

Analytical method: The first method begins with the calculation of the reciprocal lattice vector 2.7, that is given by the Miller's indexes of the lattice plane under consideration. This vector can be described in Cartesian (x, y, z) or in spherical coordinates R, ϑ and φ :

$$h \cdot \mathbf{a}^* + l \cdot \mathbf{b}^* + l \cdot \mathbf{c}^* = \mathbf{G} = R \cdot \begin{pmatrix} \cos(\varphi) \sin(\vartheta) \\ \sin(\varphi) \sin(\vartheta) \\ \cos(\vartheta) \end{pmatrix} \quad (2.10)$$

From part c) of FIG. 2.4 one can see the relation

$$\varrho = R \cdot \tan\left(\frac{\vartheta}{2}\right) \quad (2.11)$$

for the distance from the centre of the stereographic projection to point P . The angle φ can be used without any transformation. This method can also be used in the opposite direction i.e. when a point in the stereographic projection is given.

Meridians and parallels: Wulff net The description of meridians and parallels is done the best ways in another notation FIG. 2.5. In this changed notation a lattice plane normal can be defined by a *longitude* λ and a *latitude* ψ angle. These angles are also known from the coordinate system on the globe. Whereas *meridians* contain all poles with constant λ - these are just the great

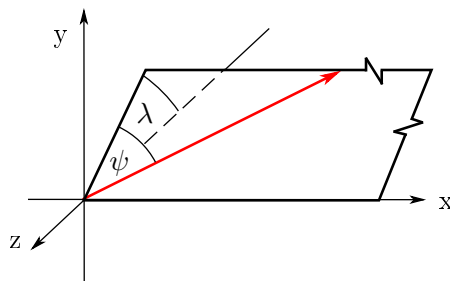


FIG. 2.5: Definition of longitude λ and latitude ψ . Take care about the change in orientation compared to the figure FIG. 2.4 for a better viewing

circles of a sphere -, the so called *parallels* are the set of poles with constant ψ . (see FIG. 2.6 for help in geometrical understanding). The meridians are same as the crystallographic *zones*.

The *Wulff net* shows the stereographic projection of several meridians and parallels with certain constant spacing in the values for λ and ψ . An implementation with a change in longitude and latitude of 5° per step is shown in FIG. 2.7.

Usage of Wulff net: Geometrical method The Wulff net is the basis of the second method that is a geometrical method. In principle it can be used for two different classes of tasks: One can draw the stereographic projection for a given set of poles or one can get angular relations between the poles in a given projection.

The first task gives more insight in the working principle of the net:

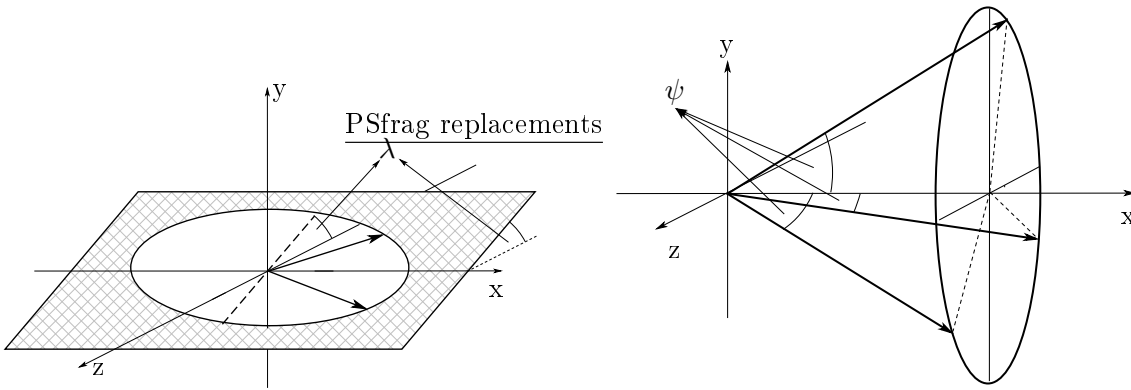


FIGURE 2.6: Meridians - poles with constant longitude λ - and parallels - pole with constant latitude ψ

- A projection is only valid for a certain orientation of the crystal. So at first the orientation of the crystal with respect to the projection plane must be known and fixed. Fixing the pole in the centre of the projection is sufficient. One says: “I draw the stereographic projection in direction (111) ”.
- The second pole in the projection - the first one was the pole in the centre - can be drawn at an arbitrary angle φ in projection plane. Only the distance from the centre is relevant for positioning the pole. This distance is in fact an angle given by (2.8) and has to be counted in units of the Wulff net, i.e. in units of meridians from the centre meridian.
- The remaining pole are entered as follows:
 - At first one has to calculate the angle towards the pole in the centre.
 - Now the Wulff net is rotated around the centre point until another known pole lies on the meridian λ that is equal to the calculated angle. Now one knows, that the known pole and the new lie on the same meridian, i.e. the two poles have the same longitude λ
 - The difference in latitude $\Delta\psi$ is the angular distance between these two pole and is calculated again with the formula (2.8). One can measure it in stereographic projection in units of crossings with the parallels in the net.

The second task is quite similar:

- To get the angular relation between two poles out of the stereographic projection, one has to rotate the Wulff net until the two poles lie on the same meridians.
- Now the angular distance is given by the change in latitude ψ from one pole to the other.

poles, that lie on the same meridian, belong to the same *zone*. If the Wulff net is orientated in such a way, that the zone condition is visible, one can also mark the *zone axis*. This zone axis is normal to the zone and the coordinates in the projection are given just the same as it is the case for a simple pole. The coordinates are: $\lambda_{\text{zone axis}} = \lambda_{\text{zone}} - 90^\circ$ if $\lambda_{\text{zone}} \geq 0^\circ$ and $\lambda_{\text{zone axis}} = \lambda_{\text{zone}} + 90^\circ$ otherwise. The other coordinate $\varphi_{\text{zone axis}} = 360^\circ - \varphi_{\text{farrest pole from centre}}$.

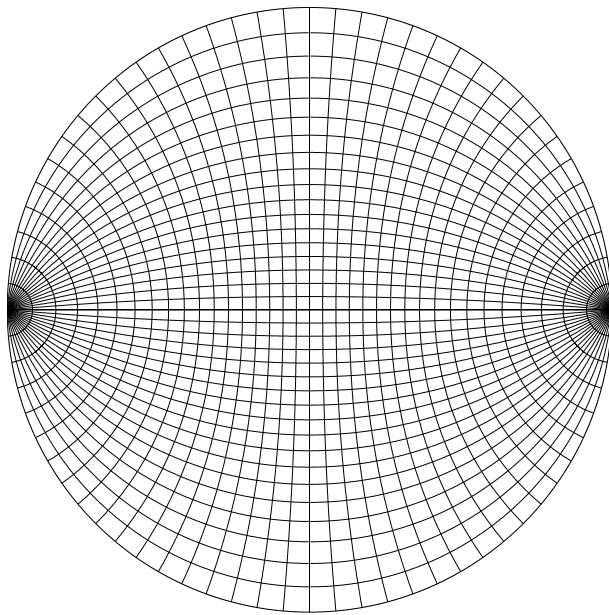


FIG. 2.7: Wulff net with divisions $\Delta\psi = 5^\circ$ and $\Delta\lambda = 5^\circ$. The orientation is $x:\rightarrow$ and $y:\uparrow$. Further implementations with various divisions in λ and ψ with different line thicknesses are linked [here](#).

Illustration of pointgroups with the help of stereographic projection: The 32 point groups build the irreducible group of combinations of symmetry operations in 3 dimensional space except the translation. The single elements of this group can be distinguished and explained by their stereographic projection. Starting from a single pole in the stereographic projection with the Miller's Indexes (hkl) the symmetry elements of the point group under consideration are applied to the pole in the projection. One gets further poles on the basis of the contained symmetry operations. If a pole is transferred to itself, one has left the *general positions* and the projection is reduced to *special positions* of the poles. If this happens the number of poles in the projection is reduced in comparison to the general positions.

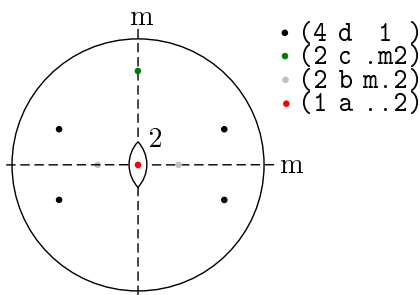


FIGURE 2.8: General (black) and special (colored) positions of the point group $mm2$

FIG. 2.8 shows the stereographic projection of the point-group $mm2$. It belongs to the orthorhombic coordinate system.

The importance of this theory for the experiment lies in the symmetry considerations, which are valid for the stereographic projection just as for the laue diffraction pattern. All symmetry elements of a point group must appear also in the diffraction pattern. The diffraction has to reveal even more symmetries as it cannot distinguish between point groups with and without an inversion. So the 32 crystallographic point groups are reduced to 11 distinguishable *Laue groups*.

This means, that the diffraction pattern of a crystal with a hexagonal unit cell will show a 6-fold rotation axes in several diffraction orders (see 3) of the Laue record is the incoming beam is perpendicular to the (001) lattice plane.

Further information and the description of all 32 point groups and their stereographic projection

can be found in [Pub89].

2.5 Crystal structures and used crystals.

2.5.1 Quartz

Quartz is nothing else than silicon oxide SiO_2 in a special crystalline structure. In contrast to gallium arsenide the constituent atoms of Quartz Si and O do not build up two Bravais lattices with a specific orientation to each other. Instead the silicon atoms represent the centres of a tetrahedra. The corners of the tetrahedra are occupied by the oxygen atoms. (see FIG. 2.9). Since the stoichiometric relation of 1 Si atome per 2 O atoms is violated for a single tetrahedra, every single oxygen atom is connected with two silicon atoms and represent the corners of two touching tetrahedra. The crystalline structure is the following: The first position of such a SiO_4 -tetrahedra may be (000). By rotation of 120° and subsequent displacement in the crystallographic c-axis one reaches the second position of a tetrahedra: $(-a/2 \sqrt{3} a/2 c/3)$. Another screw rotation leads to the third position in the unit cell: $(-a/2 - \sqrt{3} a/2 c/3)$. In FIG. 2.9 two helices with the length of 2 unit cells are shown. Combining all other atoms of the structure, one can see the hexagonal unit cell of the crystal. The lattice constants are $a = 4,9124 \text{ \AA}$ and $c = 5,40039 \text{ \AA}$.

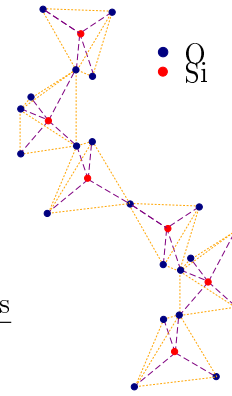
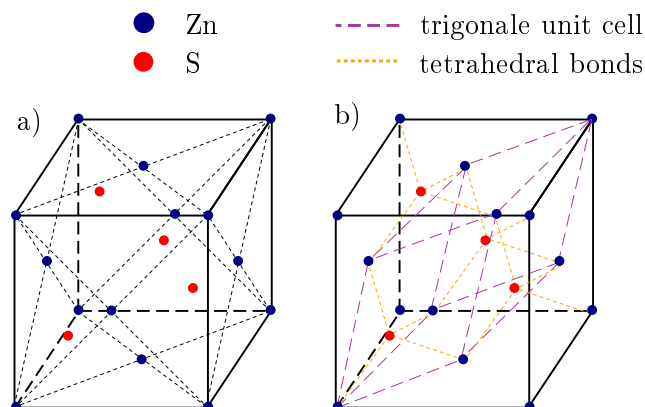


ABB. 2.9: Helixstructure of Quarz

2.5.2 Zinc blend structure

Zinc sulfate (ZnS) occurs mainly in two configurations of solid state, the wurzite- and the zinc blende structure. For the second structure the zinc atoms and the sulphur atoms build up two separate cubic face centered lattices (fcc). Moreover these two lattices are displace by $1/4$ (in units of the diagonal) along the diagonal. FIG. 2.10 shows the atomic positions of the zinc and sulphur in a single fcc unit cell of the crystal. It contains 4 zinc and 4 sulphur atoms, so the stoichiometric relation is fulfilled.

FIG. 2.10: zinc blend structure: a) shows the fcc-structure b) shows the tetraedric structure, that is typical for diamond structures.



The positions of the atoms in the unit cell in reference to the cubic basis vectors are:

$$\begin{aligned} \text{Zn:} & \quad \{(0\ 0\ 0), \quad (0\ 1/2\ 1/2), \quad (1/2\ 0\ 1/2), \quad (1/2\ 1/2\ 0)\} \\ \text{S:} & \quad \{(1/4\ 1/4\ 1/4), \quad (1/4\ 3/4\ 3/4), \quad (3/4\ 1/4\ 3/4), \quad (3/4\ 3/4\ 1/4)\} \end{aligned} \quad (2.12)$$

Another example for the zinc blend structure ist Gallium arsenide, which is used in this experiment. The cubic lattice constant is $a = 5,6533 \text{ \AA}$. Further information on this crystal can be found in [\[Wik\]](#).

The diamond lattice is a special type of a zinc blend structure, as for diamond both types of atoms are the same. Carbon, silicon and germanium can crystallise in this configuration.

Further literature to this topic can be found in [\[Dem05\]](#), [\[Kle98\]](#) and in [Kristallographie I](#) von Walter Steurer and Thomas Weber. Unfortunately, these books are written in german. However, there will also be much literature in English language.

3 X-ray diffraction at crystals

3.1 Simple diffraction theory

For this section the standard literature of solid state physics is useful.

The *simple diffraction theory* of X-rays is based on the following physical process: An *incoming plane wave* with a wavevector \mathbf{k}_o ($|\mathbf{k}_o| = k = 2\pi/\lambda$) enters matter and induces the atomic electrons to oscillations of the same frequency as the incoming wave. These oscillations give rise to the emission of spherical waves. The intensity of the superposition of all scattered waves is observed at an observation point B. The direction from the interaction point to this point is given by the wavevector \mathbf{k} of the outgoing wave. Since the refractive index of matter and air is nearly 1 for X-rays, one can state $|\mathbf{k}| = k$. The amplitude of the incoming wave at point P in matter is given

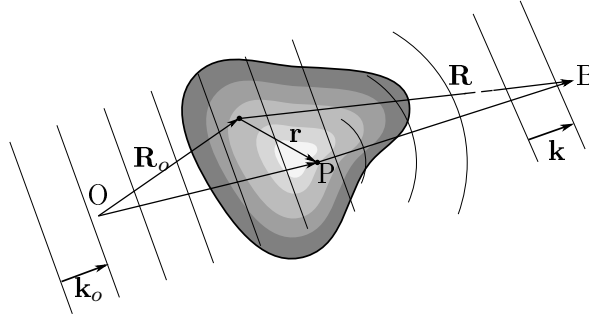


FIG. 3.1: Simple diffraction theory

by:

$$A_P(\mathbf{r}, t) = A_o \cdot e^{i\mathbf{k}_o \cdot (\mathbf{R}_o + \mathbf{r}) - i\omega_o t} \quad (3.1)$$

Here \mathbf{R}_o is the leading vector to the sample. At point P an electron is excited and emits a spherical wave with a probability f . The amplitude of this wave at point B can be approximated by

$$A_B = A_P(\mathbf{r}, t) \cdot f \cdot \frac{e^{ik \cdot (\mathbf{R} - \mathbf{r})}}{R} \quad (3.2)$$

In order to calculate the amplitude of all diffracted wave at point B one has to integrate of the total scattering volume of the sample. The spatial weighting is done by a spacial depending *electron density distribution* $\varrho(\mathbf{r})$. Hence the integrated intensity at the observation point - only this quantity is measurable in the experiment - is given by:

$$I_B^{\text{Gesamt}} = \frac{A_o^2}{R^2} f^2 \cdot \left| \int_{\text{Streu-}}^{\text{volumen}} \varrho(\mathbf{r}) e^{i(\mathbf{k}_o - \mathbf{k}) \cdot \mathbf{r}} d^3r \right|^2 \quad (3.3)$$

Furthermore the charge density distribution shows the same periodicity like the crystal lattice. Thus one can develop this function into a series of reciprocal lattice vectors.

$$\varrho(\mathbf{r}) = \sum_{\mathbf{G}} \varrho_{\mathbf{G}} \cdot e^{i\mathbf{G} \cdot \mathbf{r}} \Leftrightarrow \varrho_{\mathbf{G}} = \frac{1}{V_{\text{EZ}}} \cdot \int \varrho(\mathbf{r}) \cdot e^{-i\mathbf{G} \cdot \mathbf{r}} d^3r \quad (3.4)$$

The sum of the series is independent from the integral in (3.3), so detach this sum from the total integral and one gets for the remaining integral:

$$\int e^{i(\mathbf{G}-\mathbf{q})\cdot\vec{r}} d^3r = \begin{cases} V & \text{für } \mathbf{G} = \mathbf{q} \\ 0 & \text{sonst} \end{cases} \quad (3.5)$$

The extracted *diffraction condition* is the condition for *constructive interference* of all scattered waves in point B:

$$\mathbf{q} = \mathbf{k} - \mathbf{k}_o = \mathbf{G} \quad (3.6)$$

The measurable intensity can be formulated:

$$I_B^{\text{Gesamt}} = \frac{A_o^2}{R^2} N^2 f^2 \cdot |\varrho_{\mathbf{q}}|^2. \quad (3.7)$$

3.2 The Laue equations

The multiplication of the equation (3.6) with each of the lattice base vectors \mathbf{a} , \mathbf{b} und \mathbf{c} leads to the three *Laue equations* (using equations 2.1):

$$\begin{aligned} (\hat{\mathbf{n}} - \hat{\mathbf{n}}_o) \cdot \mathbf{a} &= h \cdot \lambda \\ (\hat{\mathbf{n}} - \hat{\mathbf{n}}_o) \cdot \mathbf{b} &= k \cdot \lambda \\ (\hat{\mathbf{n}} - \hat{\mathbf{n}}_o) \cdot \mathbf{c} &= l \cdot \lambda \end{aligned} \quad (3.8)$$

Here the relations $\hat{\mathbf{n}} = \frac{\mathbf{k}}{k}$ and $\hat{\mathbf{n}}_o = \frac{\mathbf{k}_o}{k_o}$ can be applied. In the experiment $\hat{\mathbf{n}}$ and $\hat{\mathbf{n}}_o$ can be determined directly from the Laue records. So the Laue equations deliver three conditions for the four unknown quantities h , k , l and λ . A solution to this problem is not accessible without further information about the unknown parameters. Fortunately it is known, that h , k und l are integer numbers. Therefore

$$h = \frac{(\hat{\mathbf{n}} - \hat{\mathbf{n}}_o) \cdot \mathbf{a}}{(\hat{\mathbf{n}} - \hat{\mathbf{n}}_o) \cdot \mathbf{c}} \cdot l \quad \text{and} \quad k = \frac{(\hat{\mathbf{n}} - \hat{\mathbf{n}}_o) \cdot \mathbf{b}}{(\hat{\mathbf{n}} - \hat{\mathbf{n}}_o) \cdot \mathbf{c}} \cdot l \quad (3.9)$$

must result in integer numbers, if l is chosen to be integer. Using this information, one can determine all four unknown parameters, if the orientation of the crystalline unit cell i.e the cartesian representations of \mathbf{a} , \mathbf{b} and \mathbf{c} in the laboratory coordinate system are known.

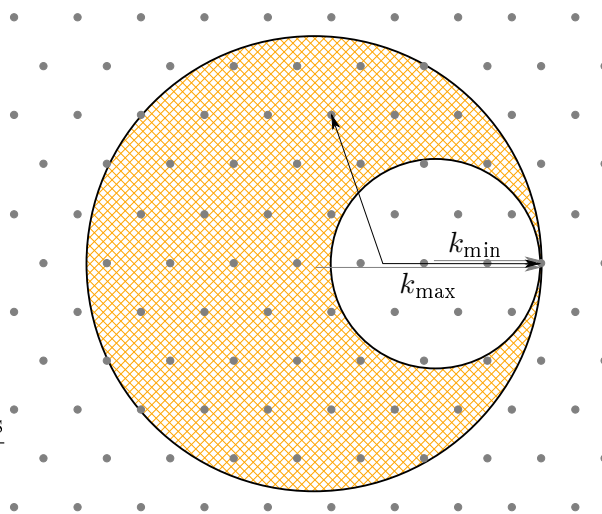
3.3 Ewald construction and the reciprocal space

The diffraction condition (3.6) can be interpreted geometrically using the *Ewald construction*:

- In this experiment the crystal is irradiated with polychromatic X-rays Therefore the absolute value of the wave vector $k = |\mathbf{k}| = |\mathbf{k}_o|$ can take all values in the interval $k \in [k_{\min}, k_{\max}] = [2\pi/\lambda_{\max}, 2\pi/\lambda_{\min}]$. Whereas λ_{\min} is determined by (1.6) and the maximum kinetic energy of the accelerated electrons (in the case of X-ray tubes) λ_{\max} is limited only by the decrease of intensity with higher wavelengths.

- The *reciprocal space* is a 3dimensional space that is build up by the reciprocal lattice base vectors (2.2). It contains the reciprocal lattice of the crystal and has the same units like k (compare with 3.6). Hence, one it makes sense to draw the wave vectors of the incoming and outgoing beams into the reciprocal space.
- FIG. 3.2 shows the ewald construction in 2 dimensions. Two circles with the radii k_{\min} and k_{\max} are drawn in such way, that the cross each other in a single point of the reciprocal lattice. The connection lines between the centre and this reciprocal lattice point have to be parallel to each other and parallel to the direction of the incoming beam.
- The diffraction condition is now fulfilled for all reciprocal lattice vectors, that connect the crossing point of the two circles with another lattice point in between the two circle and the two spheres in 3D respectively. This is shown for a single set of incoming and outgoing wave vector and a reciprocal lattice vector.

FIG. 3.2: Ewald construction: The lengths of the shown wave vectors are k_{\min} , k_{\max} and $k_{\min} < k < k_{\max}$. All reciprocal lattice points inside the cross hatched area lead to a constructive interference in the corresponding directions.



3.4 Bragg's interpretation of the diffraction condition

Bragg interpreted the diffraction condition 3.6 as a constructive interference at the lattice planes of the crystals. The incoming X-ray beam is deflected like an optical beam optics according to the well known reflection law: Is the difference in the optical length of the different paths through the crystal in FIG. 3.3 just a integer multiple of the wavelength, the condition for constructive interference is fulfilled.

The difference in the optical path lengths is given by:

$$m \cdot \lambda = \Delta s = 2 d_{hkl} \cdot \sin(\vartheta) \quad (3.10)$$

d_{hkl} is the distance between two neighbouring lattice planes, that can be calculated by means of equation (2.9). m is a integer number and counts the order of the interference. In this case of Laue diffraction of X-rays one can approximate the refractive index by $n \approx 1$.

It is possible to show the equivalence of the Laue equations (3.8) and Bragg's equation (3.10) in general.

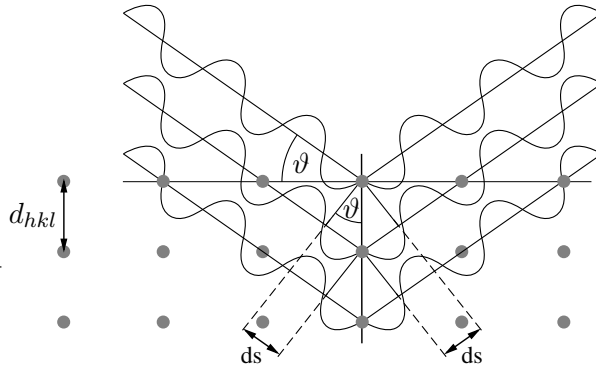


FIG. 3.3: Bragg's interference condition: The incoming beam encloses an angle ϑ with the lattice plane

3.5 Atomic form factor, structure factor and extinction rules

The scattered intensity in (3.7) depends on the absolute square of the Fourier transformed component of the charge density distribution $\varrho_{\mathbf{G}}$. Here \mathbf{G} is just the reciprocal lattice vector for which a constructive interference is observed. The integration 3.4 is done over the volume of the total unit cell of the crystal.

Moreover it is possible to understand the total charge density as the sum of charge densities of all atoms in the unit cell with the origin at the coordinates of the atoms \vec{r}_α : $\vec{r} = \vec{r}_\alpha + \vec{r}'$:

$$\begin{aligned}\varrho_{\vec{G}} &= \frac{1}{V_Z} \int_{\text{Zelle}} \sum_{\alpha} \varrho(\mathbf{r}_\alpha + \mathbf{r}') \cdot e^{-i\mathbf{G}\cdot\mathbf{r}' - i\mathbf{G}\cdot\mathbf{r}_\alpha} d^3r' \\ &= \frac{1}{V_Z} \sum_{\alpha} e^{-i\mathbf{G}\cdot\mathbf{r}_\alpha} \cdot \underbrace{\int \varrho_{\alpha}(\mathbf{r}') \cdot e^{-i\mathbf{G}\cdot\mathbf{r}'} d^3r'}_{f_{\alpha}}\end{aligned}\quad (3.11)$$

f_{α} is the *atomic form factor* of the different atoms. The total sum is called *structure factor* of the crystal. The only free parameters are the components of the reciprocal lattice vectors \mathbf{G} and the Miller's indexes respectively.

$$S_{\mathbf{G}} = \sum_{\alpha} f_{\alpha} \cdot e^{-i\mathbf{G}\cdot\mathbf{r}_\alpha} \quad (3.12)$$

$$(3.13)$$

The atomic form factor f_{α} defined in (3.11) can be calculated for an angle θ between \vec{G} and \vec{r}' and a radial symmetric potential:

$$f_{\alpha} = \int \varrho_{\alpha}(\mathbf{r}') e^{-i\mathbf{G}\cdot\vec{r}'} d^3r' \quad (3.14)$$

$$\begin{aligned}&= -2\pi \int_0^{\infty} \int_{-1}^1 \varrho_{\alpha}(r') e^{iGr' \cdot \cos(\theta)} r'^2 d' d \cos(\theta) \\ &= 4\pi \cdot \int_0^{\infty} \varrho_{\alpha}(r') \cdot r'^2 \cdot \frac{\sin(G \cdot r')}{G \cdot r'} dr'\end{aligned}\quad (3.15)$$

As an example the structure factor of a cubic face centred crystal with a single type of atoms can be expressed by:

$$S_{\mathbf{G}}^{\text{fcc}} = f \cdot \left(1 + e^{\pi i (h+k)} + e^{\pi i (k+l)} + e^{\pi i (l+h)} \right)$$

Obviously, $S_{\mathbf{G}}^{\text{fcc}}$ vanishes, if two of the integer numbers h , k and l are even. *Extinction rules* like this and many others arise in dependence from the distribution of the atoms in the unit cell and the relative values for the form factors of different atoms in the unit cell.

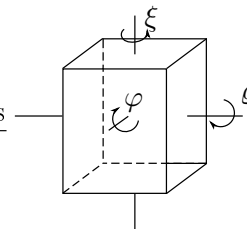
Further information can be found in [Dem05] and in [Physik der Röntgenstrahlung](#).

4 Versuchsbeschreibung

The experimental setup, procedure and tasks will be explained in this section. It is obligatory, that the students comply with the mentioned safety and operation instructions.

4.1 Experimental tasks

This section begins with the description of the experimental tasks that has to be executed in this experiment. The various elements not mentioned in the theoretical part are explained in the following. A careful protocol of the experimental steps is of elementary importance. It is no problem to draw another sketch, on the other side a missing information mostly is not accessible after finishing the experiment.



Determination of the orientation of a crystal : At first the two Imageplates (IP) has to be erased and read out to be sure, that the are more signals stored in them. To guarantee this one should do a test readout of the IPs. It's important to handle the IPs with care. Therefore they must only be moved with a small sucker.

A alpha-quartz crystal will be mounted on the sample holder of the Laue camera and adjusted in such a way, that all angles of the goniometer show a value of 0° .

The camera will be equipped with the erased IPs in direction of reflection and transmission. The illumination is done with a collimator diameter of 0.8 mm for 8 Minutes at a current of 30 mA and a acceleration voltage of 40 kV. It is very important, that the IP carrier of the camera is put together and mounted correctly. A comparison with the record of an orientated sample from FIG. 4.1 should be done.

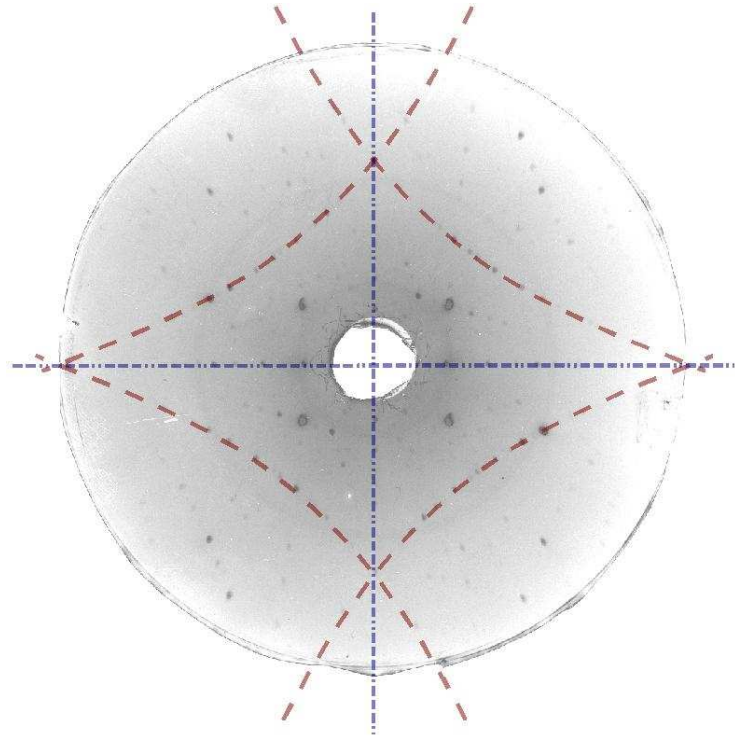
The aim of this task is to re-adjust the orientation of the crystal to its (110)-lattice plane. The following steps have to executed:

- High symmetric reflexes has to be extracted and identified from the first record with the help of the Greninger net. The characteristics of such high symmetric reflexes is that many zones cross each other in theses points. Furthermore the are only few reflexes in the direct vicinity of these symmetric reflexes. The identification of these reflexes is done by a measurement of the angluar distances to each other with the Greninger net in comparison with theoretical angles between low indexed lattice planes, i.e. reflexes with Millers indices h, k, l in the range of $\{-1, 0, 1\}$. It is advisable to prepare a table of all these angles before starting the experiment. Moreover a measurement of the distance sample to screen is necessary for the choice of the correct Greniger net.
- The orientation of the crystal is adjusted with the following iterative method. After each record out of a series of about 3-5 illuminations the deviation of the (110)-reflexes from the center of the record in λ and ψ has to be measured. Now alternately one of these two deviation angles is translated into a rotation of the sample with the goniometer. After every variation another record has to be done. The first record should lead to correction of the ψ angle.
- A trouble-free and efficient experimental development is garantueed by a rigorous erasing of the IPs after each read out. This can be reached by exposing the IP to moderate

sunlight for about 10 minutes. Obviously it is useful to change the IP from one record to the other in order to shorten waiting times.

- In the end of the orientation process the (110)-reflex must not deviate more than 1° in λ and ψ from the center of IP. Careful protocoling of the different records is obligatory. Especially the orientation of the IP in the Laue camera has to be well-known.

FIG. 4.1: Laue record of a SiO_2 crystal in direction of reflection. The incident beam is parallel to the (110) surface pole. The red marked meridians are symmetry equivalent. The meridian located mostly in the 1st quadrant contains the following poles: (11-1), (0-10), (10-1), (-1-1-1). The crossings of this meridian with the blue horizontal meridian and the blue vertical meridian are the (0-10) and the (-1-1-1) poles, respectively.



Calculation of Miller's indexes out of a laue record: A part of a GaAs Wafer has to be adjusted to its polished (111)-surface. Determine the Miller's Indexes of the clearly visible Laue Spots in the reflection pattern of GaAs. Furthermore the corresponding wavelengths should be calculated. Think about a reasonable error treatment. Proceed in the following way:

- Define the axis of the laboratory system. Choose this system in such a way, that some spots lie on the x or y-axis.
- Calculate the normalized direction vectors $\hat{\mathbf{n}}_i$ from all reflection spots in the pattern - leading from the crystal to spots in the laboratory system and vector of the incoming beam $\hat{\mathbf{n}}_o$.
- Define the base lattice vectors of the crystal system. determine the transformation Matrix \mathcal{M} from the crystal system to the laboratory system:

$$\mathbf{r}_{\text{LS}} = \mathcal{M} \cdot \mathbf{r}_{\text{CS}}$$

Use the fact, that the crystal surface is not only a (111) lattice plane, but also perpendicular to the direction of the incoming beam.

Is there a freedom left in the definition of \mathcal{M} ?

- Transform the lattice base vectors from the crystal system representation to the laboratory system representation and calculate the values:

$$h' = \frac{(\hat{\mathbf{n}}_i - \hat{\mathbf{n}}_o) \cdot \mathbf{a}}{(\hat{\mathbf{n}}_i - \hat{\mathbf{n}}_o) \cdot \mathbf{c}} \quad k' = \frac{(\hat{\mathbf{n}}_i - \hat{\mathbf{n}}_o) \cdot \mathbf{b}}{(\hat{\mathbf{n}}_i - \hat{\mathbf{n}}_o) \cdot \mathbf{c}}$$

for each reflection spot.

- Calculate the Millers Indexes h, k, l from the values h' and k' for the spots and the corresponding wavelengths λ .
- Do an error discussion leading to estimations on the error of h, k, l and λ . This can be done while dealing with the other parts of this task or in the end.

Analysis of a film record of a quartz crystal in transmission The Quartz crystal of the first task will be placed inside the Laue-Camera with an arbitrary orientation. Light sensitive photofilms will be installed in direction of reflection and transmission and illuminated for about 10 hours. After the development of the films in the photo laboratory, several reflexes have to be transferred to a transparency. Extract 7 meridians with the help of the Leonhardt net and transfer the corresponding lattice poles to the Wulff net (stereographic projection). The positions of the single reflexes on the meridians have to be transferred, too. In which area of the stereographic projection do you find the reflexes of the transmission record, where the reflexes of the reflection record?

4.2 Elements of the experiment

4.2.1 Safety warnings and instruction rules

- The laser can only be used with suitable safety or adjustment glasses.

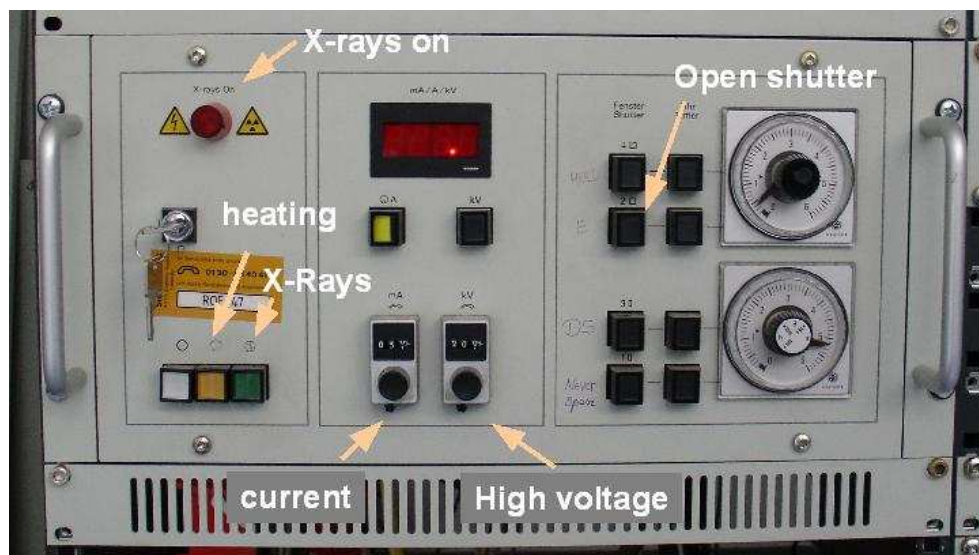


ABB. 4.2: Usage of the X-ray system

- it's not allowed to open the doors of the X-ray rack before switching off the power supply of the x-ray tube. Opening the X-ray rack without switching off the power supply will cause an emergency shut down of the power that can probably damage the system.
- However, the system will react with an emergency shutdown, if the rack is not opened in accordance with the regulations. So there is no possibility for enhanced radiation exposition. It is not allowed to switch on the power supply by deactivation of the security measures.
- In order to prevent a damage of the X-ray system the high voltage has to be increased in small steps like $0.1/kVs$. The same is true for the current: $0.1/mAs$
- At the beginning of the experiment, the X-ray system is in the heating mode. Before switching on the power supply, one should check the values of the high voltage and the current: $V_{min} = 20 kV$ and $I_{min} = 5 mA$. After turning on the voltage the voltage has to be increased up to a value of $U_{max} = 40 kV$. After that the electron current will be increased to a level of $I_{max} = [30] mA$. For shutting down the system the described procedure is reversed.

4.2.2 Laue-camera

In FIG. 4.3 one can see a photo of the Laue camera together with the goniometer and the sample crystal. In the direction of reflection one can see a plate, which contains the X-ray film of the image plate. Moreover the connection to the X-ray tube is shown.

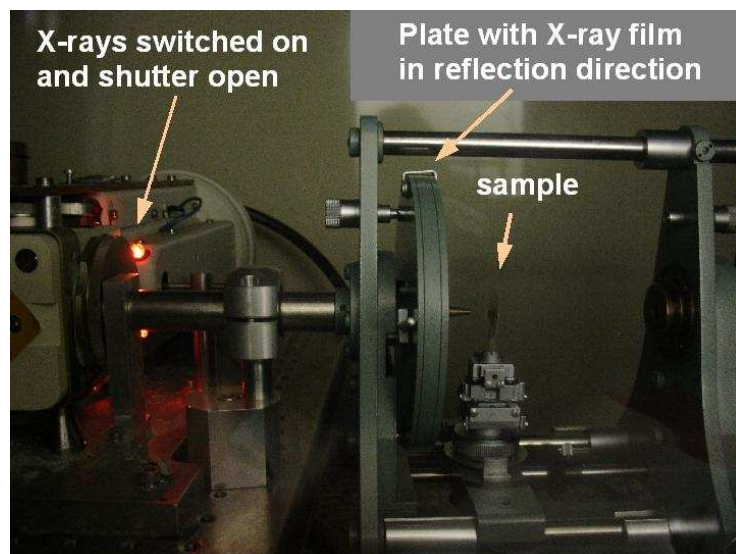


FIG. 4.3: Laue-Kamera

4.2.3 Laserjustierung

The laser adjustment of the crystal surface is done with a metal plate, that contains a laserpointer and a photo diode. The laser beams is reflected directly onto the sensitive area of the photo diode, if the distance to the sample and the orientation of the crystal surface is chosen correctly. The power supply (10 V) is connected with the blue (-) and the red (+) connection pin. The

yellow led must shine otherwise the photodiode might be damaged. Therefore the polarity of the power supply has to be checked with the multimeter. After that the multimeter is connected with the green and yellow connector pins. This signal is nearly proportional to the intensity of the incoming light. A first adjustment is done with the help of the eye. After that the orientation of the crystal has to be varied in such a way, that the voltage on the multimeter is maximal.

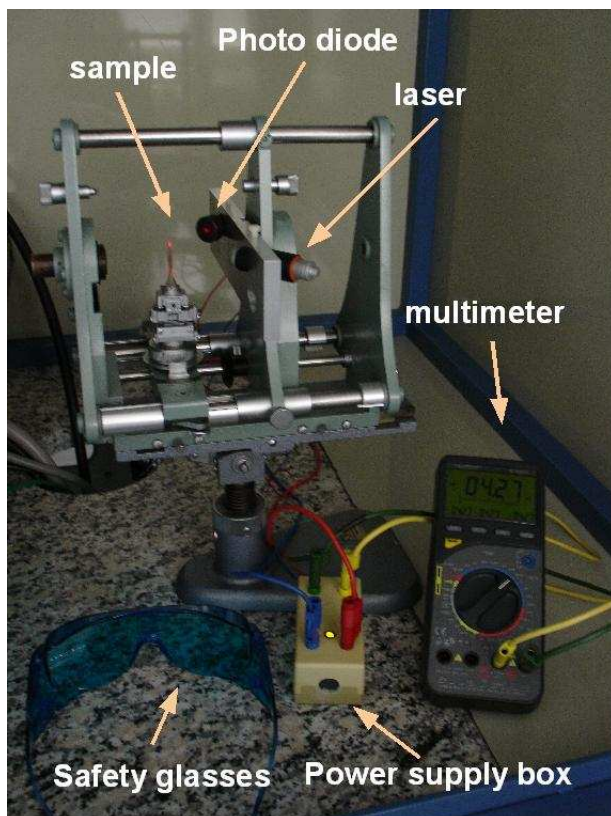


FIG. 4.4: Laser adjustment of the crystal surface

4.2.4 Projektionen der Reflexe

The Laue records can only be analysed, if the projection of the Reflexes on the detection plane is understood. At first \vec{k} is defined by (3.6) for a certain lattice plane.

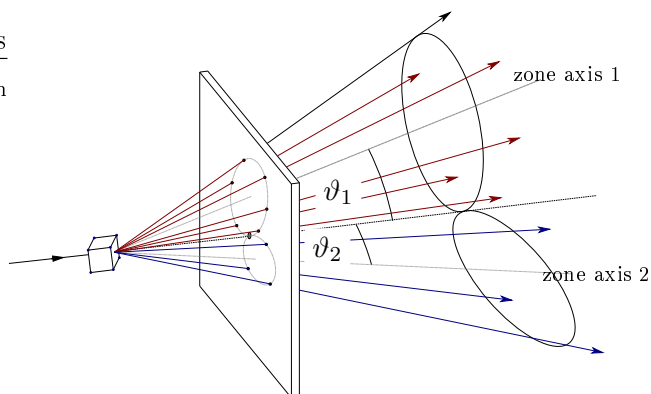
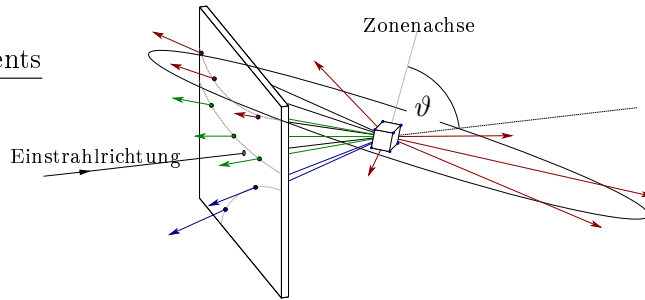


FIG. 4.5: Geometry of the transmission direction: The spots on the screen can be classified to one of the two meridians shown.

FIG. 4.6: Geometry of the reflection direction: One can see the Laue spots of three different meridians. The shown zone axis and its angle to the incident beam direction ϑ corresponds to the upper of the three meridians.



The projection of the laue reflexes on the screen is quite simple. However, not the reflexes are of interest, but the corresponding poles. In order to get the coordinates λ and ψ of the plane poles, one has to consider an additional distortion. Just as it was comfortable to use the Wulff chart for the work within the stereographic projection, it is now also useful to create a chart showing the lines, that would contain Laue reflexes of equal longitude and latitude in one chart. It is important to realize, that in contrast to the Wulff chart it is not important to choose the correct sample-film-distance for the chart. In the case of the reflection one has to use the *Greninger*- , in case of the transmission the *Leonhardt*-chart (FIG. 4.7). The parametrisation of the curves and further details are derived in the reference [Ber65]. FIG. 4.5 and FIG. 4.6 give an impression on the geometry of the projections.

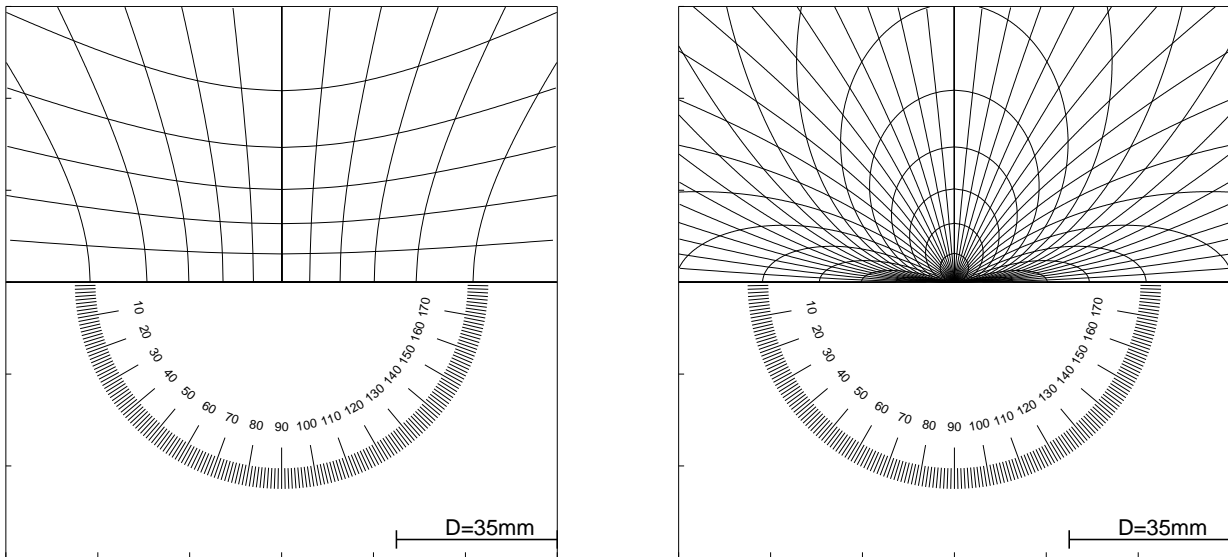


ABB. 4.7: Greninger- (left) und Leonhardt chart (right). the inner structures correspond to $\lambda = \psi = 0^\circ$ for the Greninger chart and $\lambda = 90^\circ, \psi = 0^\circ$ for the Leonhardt char.

The distance of the sample to the screen is $|D| = 35 \text{ mm}$.
The connection between the real coordinates of the stereographic projection and the two charts

are depicted in FIG. 4.8 and FIG. 4.9. The corresponding transformations are given by:

Reflection direction:

$$D < 0$$

$$\vartheta = \frac{1}{2} \cdot \arctan\left(-\frac{r}{D}\right) \quad (4.1)$$

$$\rho = \tan\left(\frac{\vartheta}{2}\right)$$

$$= \tan\left[\frac{1}{4} \cdot \arctan\left(-\frac{r}{D}\right)\right] \quad (4.2)$$

Transmission direction:

$$D > 0$$

$$\vartheta = \frac{\pi}{2} - \frac{1}{2} \cdot \arctan\left(-\frac{r}{D}\right) \quad (4.3)$$

$$\rho = \tan\left(\frac{\vartheta}{2}\right)$$

$$= \tan\left[\frac{\pi}{4} - \frac{1}{4} \cdot \arctan\left(-\frac{r}{D}\right)\right] \quad (4.4)$$

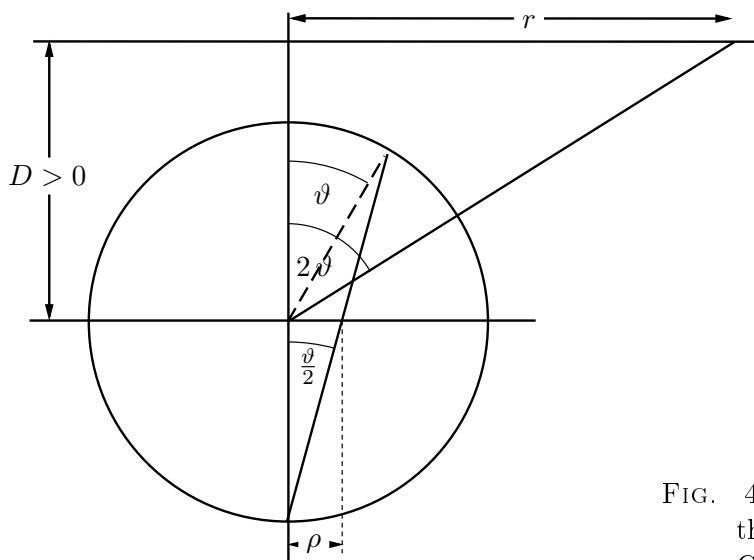


FIG. 4.8: Calculation of the coordinates in the Greninger chart

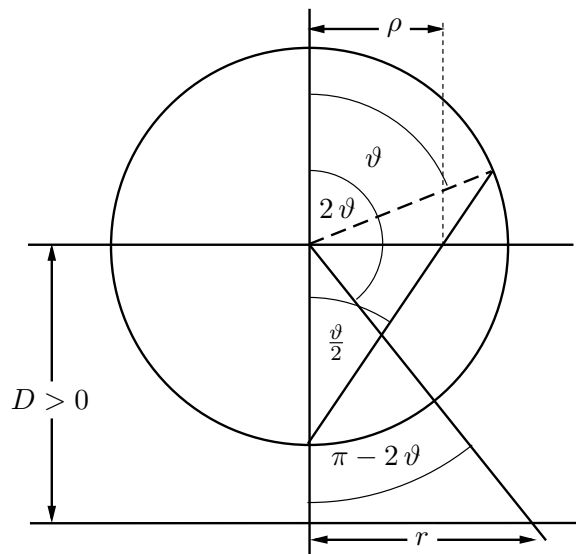


FIG. 4.9: Calculation of the coordinates in the Leonhardt chart

4.2.5 Filmentwicklung und Imageplate-system

X-ray film development The film development is done in a dark room with the help of common development and fixing baths. The time for development adds up to approximately 1 minute, the fixing is done in 7 minutes. After that the film is washed out in water for about 20 minutes and dried for 45 minutes.

Imageplate-system One has to stick to the [operation manual](#) in order to prevent damage of the system.

4.2.6 Literature of comparable experiments (german)

Further literature is linked in the following list:

- Alexander Heide: [Debye-Scherrer-Verfahren und Laue-Verfahren](#)
- Tim Haupricht und Matthias Heidemann: [Röntgenographische Methoden](#)
- Carola Eyßell und Tim-Oliver Husser: [Kristallzucht und Röntgenbeugung](#)

5 References

- [Ber65] BERNALTE, B.: *On the Curves in the Greninger and Leonhardt Nets*. *Acta Crystallographica*, 1965.
- [Dem05] DEMTRÖDER, WOLFGANG: *Atome, Moleküle und Festkörper*, 2005.
- [Gru94] GRUPEN, CLAUS: *Particle detectors*, 1994.
- [Kle98] KLEBER, WILL: *Einführung in die Kristallographie*, 1998.
- [Lau13] LAUE, FRIEDRICH, KNIPPING. *Annalen der Physik*, 1913.
- [Pub89] PUBLISHERS, KLUWER ACADEMIC: *International Tables for Crystallography, Volume 1*, 1989.
- [Wik] WIKIPEDIA: *Galliumarsenid, Quarz*. www.wikipedia.de.